

Study Optimization of a Hybrid Solar-Wind System from an Individual in Ouagadougou

Abdoulaye Compaore¹, Boukaré Ouedraogo², Kayaba Haro¹, Rimnogo Wilfried Ouedraogo¹, Yassia Belem³, Oumar Sanogo¹

¹Institute of Research in Applied Sciences and Technologies (IRSAT/CNRST), Ouagadougou, Burkina Faso

²Norbert ZONGO University, Koudougou, Burkina Faso

³University Joseph KI-ZERBO, Ouagadougou, Burkina Faso

Email: compadoul2003@yahoo.fr

How to cite this paper: Compaore, A., Ouedraogo, B., Haro, K., Ouedraogo, R.W., Belem, Y. and Sanogo, O. (2022) Study Optimization of a Hybrid Solar-Wind System from an Individual in Ouagadougou. *Open Journal of Applied Sciences*, 12, 1796-1808. <https://doi.org/10.4236/ojapps.2022.1211124>

Received: September 23, 2022

Accepted: November 6, 2022

Published: November 9, 2022

Copyright © 2022 by author(s) and Scientific Research Publishing Inc. This work is licensed under the Creative Commons Attribution International License (CC BY 4.0).

<http://creativecommons.org/licenses/by/4.0/>



Open Access

Abstract

This work is a contribution to the study of hybrid systems for converting solar and wind energy into electricity in Burkina Faso. The approach consists of evaluating and analyzing the production of a wind turbine and a solar field in order to optimize the production of all the technologies. The results obtained made it possible to evaluate the operating performance of the installation and to show the complementarity between the two energy sources with regard to temporary and seasonal variations in resources. During nighttime periods or periods of low sunlight, the wind turbine is a good alternative to energy storage by batteries, the output of the wind turbine can be up to 853.76 W. It was also a question of proposing solutions for optimizing the hybrid system through the automation of the hybrid charge regulator. A minimum height of 30 m above the ground has been chosen as the optimum height for the wind turbine.

Keywords

Global Solar Flux, Hybrid System, Energy Conversion, PV-Wind Turbine, Automation

1. Introduction

Energy is essential and unavoidable for the socio-economic development of populations. In Burkina Faso, as everywhere in the world, it is produced mainly from fossil energy sources, whereas these sources constitute an indisputable factor of environmental pollution [1] [2] [3] [4]. Renewable energies present themselves as an adequate alternative for the production of clean and environmental-

ly friendly energy instead of fossil fuels, thus reducing their harmful impacts.

In addition, the national electricity company Burkina Faso is unable to meet the demand for electrical energy, which increases each year by around 12%. It is therefore urgent to find other alternatives to contribute to the production of electricity in the country while polluting the environment less [5] [6]. In order to overcome this energy deficit, the Burkina Faso government has embarked on a vast energy mix policy dominated by solar energy.

However, the high investment cost of solar installations, especially the storage park, is hampering the development of the sector. While 60% of the country has still unexploited wind deposits between 30 and 80 meters above sea level, with an average annual wind speed between 4.5 m/s and 7 m/s [7], these values are more interesting during periods of low sunlight or in the absence of sunlight.

The observation of the respective seasonal characteristics of the two sources of energy (wind and solar) do not compete with each other but on the contrary can enhance each other. There is a need to control the deposit of these energy sources throughout Burkina Faso and especially their mode of exploitation for a sustainable development of the sector [8] [9]. It is on the strength of this observation that we study in this article a solar-wind hybrid energy system in order to propose optimization solutions.

To carry out this study, we will first describe the system and the parameters for evaluating its electrical performance. Then we will conduct an experimental study before analyzing the results obtained.

2. Technical Description

The hybrid system studied consists of a wind turbine, a hybrid charge controller, solar panels, DC/AC converter and a storage farm [10] [11].

2.1. The Wind Turbine

This element has a diameter of one (1) meter and has a power of 1600 W. The alternator consists of permanent magnet or Permanent Magnet Generator (PMG) and is from the manufacturer "MISSOURI". The wind turbine has 9 blades covering the entire surface of the wheel and has the advantage of starting for low wind speeds, the wind turbine studied starts when the wind speed reaches 2.5 m/s. The wind engine is located at a height of 9.75 m from the ground. It is fixed to a slab by means of a 7 m stainless steel tube.

2.2. The Solar Panels

The system is composed of two (2) 250 Wp polycrystalline silicon photovoltaic panels mounted in parallel. They face west and are inclined following the slope of the house.

2.3. The Hybrid Charge Controller

The hybrid charge regulator consists of a circuit for rectifying the three-phase

alternating current produced by the wind turbine into a direct current of 24 V, a manual control system for the wind turbine and a charging circuit for the panels, all connected to a 24 V/DC bus. The bus charges the tank farm via two sources, one coming from the wind turbine and the other from the solar modules. A device takes information on the state of charge of the batteries and transmits it to the bus in order to send the current necessary for an optimal charge of the batteries. Next to all this device, there is a diversion circuit for the excess energy produced by the installation. If the batteries are fully charged and the energy supply exceeds the demand, this circuit absorbs the excess energy produced by the installation, it is made up of two resistors with a total power of 600W, model 340W2R9.

2.4. The Manual Control System of the Wind Turbine

This system (**Figure 1**) consists of a box fitted with a lever. According to his appreciation, the user can block the blades (“break” position), start the wind turbine (“run” position) or run the turbine empty (“free” position). The immediate consequences of these maneuvers can be a forced shutdown of the turbine when the maximum wind speed is not reached 20 m/s; poor energy production efficiency of the turbine; or a risk of destroying the alternator if the control remains in the “free spin” position for a long time.

2.5. DC/AC Converters

All the loads in the house use alternating current and this is possible thanks to two converters of 1500 W each. One of the converters is used for the socket circuit and the other is used for lighting and ventilation. The storage park is made up of four (4) 170 Ah lead-acid type batteries, mounted in series then in parallel so as to have a service voltage of 24 volts.

Figure 2 shows the synoptic diagram of the installation.

3. System Performance Evaluation

For the photovoltaic solar modules, the voltage and the intensity were measured by a voltmeter and an ammeter, the values collected will make it possible to evaluate instantaneous power produced using the relationship:

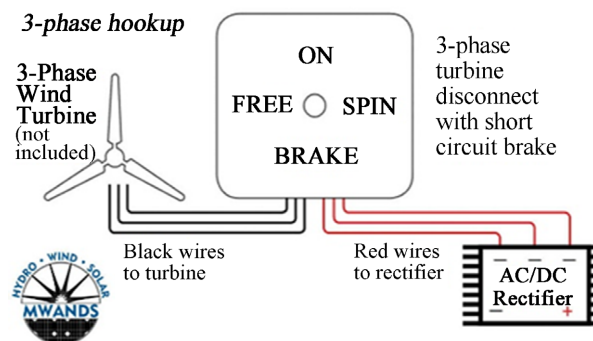


Figure 1. Wind turbine control system.

$$P = U * I \quad (1)$$

U : Voltage,

I : Current intensity.

For the wind turbine, the voltage, the intensity and the wind generation of the site will make it possible to evaluate the real operating parameters of the turbine. The voltage was measured by a voltmeter and the current was determined by Ohm's law using the shunt resistor. The parameters used in our study to evaluate the performance of the wind turbine are based on the Betz theory. Suppose the wind energy is harvested by a propeller wind motor with a horizontal axis. The propellers are placed in a fluid (air) whose upstream velocities V_{amont} and V_{aval} are non-zero with $V_{\text{amont}} > V_{\text{aval}}$. This difference in speed represents the air flow likely to be transformed by the wind turbine into mechanical power and then into electrical power as needed. This maximum power is expressed as follows [12] [13] [14]:

$$P_{\text{max}} = \frac{1}{2} \rho S (V_{\text{amont}}^2 - V_{\text{aval}}^2) \quad (2)$$

With:

ρ : density of the fluid 1.25 kg/m³;

S : area of the wind collector in m².

The kinetic energy of the fluid cannot therefore be fully recovered. **Figure 3**

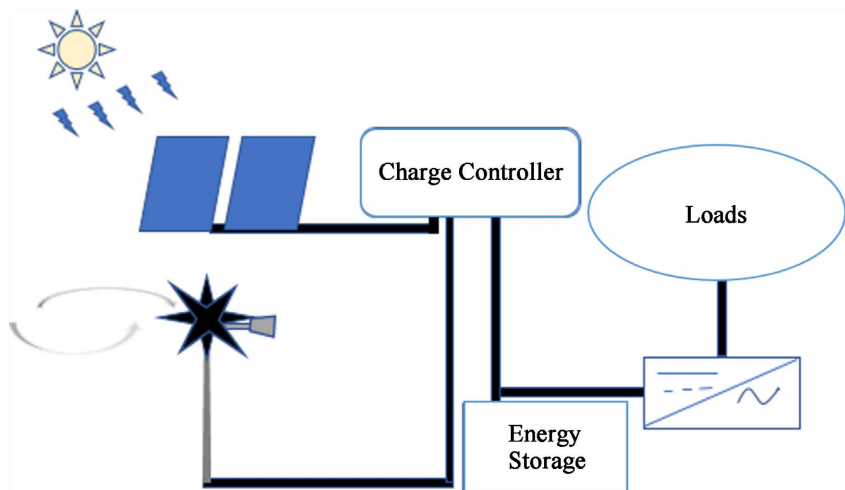


Figure 2. Synoptic diagram of the installation.

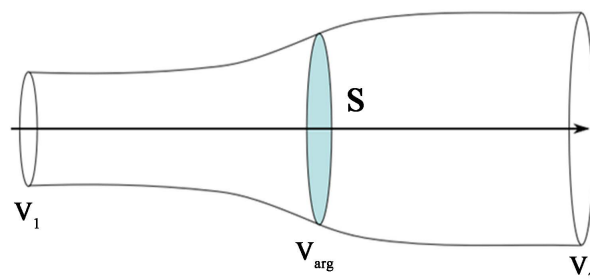


Figure 3. Stream of fluid that crosses a turbine.

illustrates a stream of fluid passing through a turbine.

The Betz limit is a physical law which indicates that the maximum theoretical incident power of the wind recoverable by a wind turbine is equal to 16/27, in fact:

$$P_{(\max)} = \frac{1}{2} \left[(\rho S (V_{\text{amont}} + V_{\text{aval}})) / 2 \right] * [V_{\text{amont}}^2 - V_{\text{aval}}^2] \quad (3)$$

$$P = \frac{16}{27} \left(\frac{1}{2} \rho S V_{\text{amont}}^3 \right) \quad (4)$$

This limit will be reached when the wind speed is divided by three between upstream and downstream of the wind turbine.

$$P_{(\text{incident})} = \frac{1}{2} \rho S V_{\text{amont}}^3 \quad (5)$$

$$V_{\text{aval}} = \frac{1}{3} V_{\text{amont}} \quad (6)$$

The incident power ($P_{(\text{incident})}$) of the wind depends on the surface that the wind sensor offers to the wind, the wind speed and the density of the air. These results can be grouped according to these formulas:

$$P_{(\max)} = \frac{16}{27} * P_{(\text{incident})} = Cp * P_{(\text{incident})} \quad (7)$$

Cp is the coefficient of performance or efficiency of the rotor. It represents the fraction of the wind energy likely to be extracted and is strongly characterized by the value of the ratio between the wind speed upstream and that downstream ($V_{\text{amont}}/V_{\text{aval}}$).

4. Experimental Study

The measurement bench set up to assess the performance of the hybrid solar-photovoltaic-wind system consists of the following equipment:

- A Graphtec midi LOGGER DL220 Datalogger to which the devices mentioned below are connected and type K thermocouples for the measurements of the desired voltages;
- A LEM HEME brand ammeter clamp, it can measure current values of up to 1000 A of all types. It has an accuracy of $\pm 1\%$ or ± 0.5 A. It was used to measure the current coming from photovoltaic solar panels;
- A Solarex brand solarimeter, it was placed in the same plane as the panels in order to determine the solar radiation they receive;
- A shunt resistor from the manufacturer METEIX, the maximum voltage and current allowed are 600 V and 30 A respectively, the resistance value is 0.01 ohm and the accuracy is $\pm 0.5\%$. It made it possible to evaluate the current produced by the wind motor through Ohm's law.
- An anemometer from the manufacturer DIGITAL ANEMOMETER can measure wind speeds of up to 30 m/s and at temperatures between -10°C and 45°C . Accuracy for wind speed measurement is $\pm 5\%$, while temperature ac-

curacy is $\pm 2\%$. It was used to measure wind speed.

The acquisition and recording of the measurements are carried out every 5 minutes.

5. Analyses and Discussions

5.1. Analysis of the Operation of the PV-Wind Turbine System

Figure 4 illustrates the evolution of the actual production of the 1600 W turbine according to the wind speed at a height of 9.75 m from the ground in the “Rimkièta” district in Ouagadougou.

We note that the wind speeds available and usable on the site during the measurement period are between 4.6 m/s and 14.2 m/s with good regularity between 7.7 m/s and 12.3 m/s. For speeds between 7.7 m/s and 12.3 m/s, the powers produced are in the range 90.4 W and 355.4 W respectively. The maximum speed recorded is 14.2 m/s for a production of 488.8 W and the minimum speed observed is 4.6 m/s with a power produced of 9.9 W. For wind speeds between 2.5 m/s and 4.6 m/s excluded, the blades of the wind turbine begin to rotate but no power is produced. This means that the alternator is only coupled to the shaft for wind speeds around 4.6 m/s.

Figure 5 shows the evolution of the power coefficient C_p of the wind turbine as a function of the ratio. It describes the evolution of the power coefficient (C_p) of the wind turbine as a function of the speed ratio. It is observed that the values of the speed ratio are between 0.85 and 2.04. The power coefficients are between 0.14 and 0.28, the maximum coefficient was observed for a ratio. It can be concluded from the parameters thus determined that the wind turbine is multi-bladed and can be classified among American wind turbines with a maximum theoretical speed coefficient estimated at 30% [14].

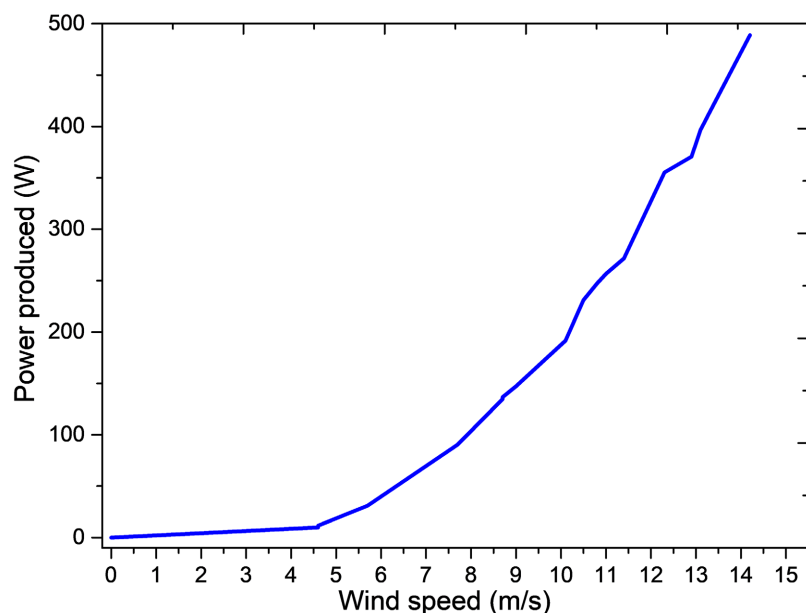


Figure 4. Evolution of the power produced according to the wind speed.

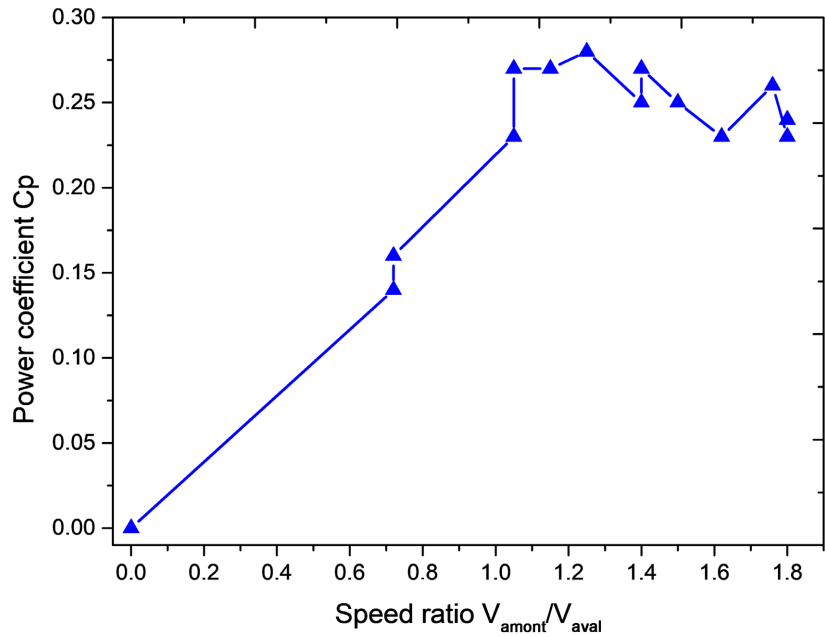


Figure 5. Evolution of the power coefficient as a function of the speed ratio.

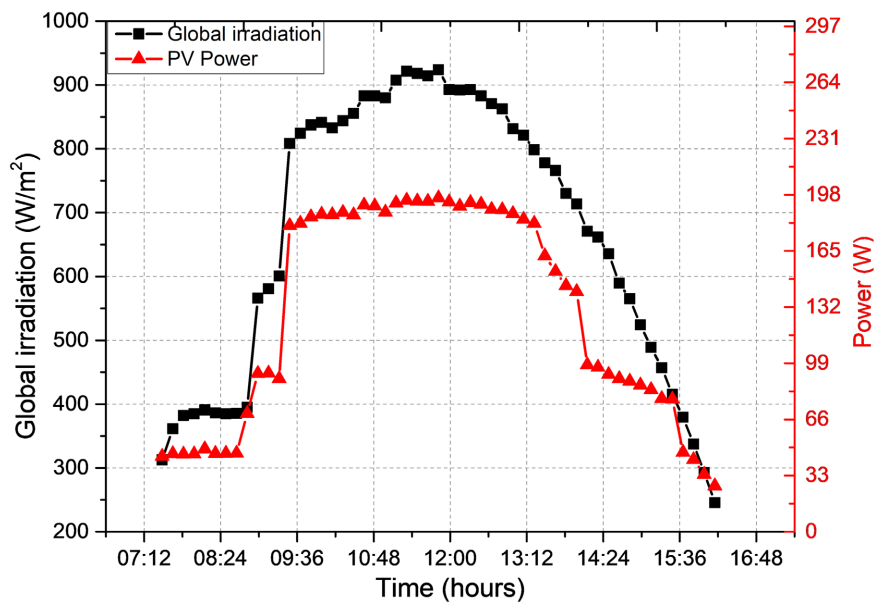


Figure 6. Evolution of the production of solar panels according to the sunshine.

The evolution of the power produced by the photovoltaic (PV) panels according to the insolation is represented in Figure 6. We note that the solar irradiation curve has a bell-shaped profile. Indeed, the curve increases from 312.5 $W \cdot m^{-2}$ to 924 $W \cdot m^{-2}$ recorded respectively at 7 h 09 min and 11 h 49 min before decreasing to 157.4 $W \cdot m^{-2}$ at 16 h 29 min. The production of solar PV modules evolves in a similar way to the curve of sunshine. It increases from 44.3 W to 196 W respectively for solar irradiation of 312.5 $W \cdot m^{-2}$ to 924 $W \cdot m^{-2}$ before decreasing to 18.3 W for sunshine of 157.4 $W \cdot m^{-2}$. The difference between the solar irradiation received by the solar panels and their production is due to the

conversion efficiency of the technology used and the production efficiency of the solar installation. Indeed, the cells of the installed solar panels use polycrystalline silicon technology. They have a relatively low yield of around 15%. In addition, this can be justified by the bad inclination (inclined according to the roof), the bad orientation of the solar panels (west face) and the bad ventilation of the panels and the absence of maintenance.

Figure 7 the overall production of the hybrid PV-wind installation. It can be seen that the total production of the hybrid system is provided solely by the solar panels from during the 9 h 39 min to 12 h 39 min range without however exceeding 200 W.

Between 12:39 and 4:39 p.m., we observe simultaneous production of the solar panels and the wind turbine. During this period, production reached a production peak of more than 937.6 W at 15 h 09 min with 85 W as production share of the PV solar modules and 853.76 W as production share of the wind turbine. This denotes a period marked by good wind activity and partially overcast skies.

During the night period 21 h 59 min to 1 h 09 min, the energy production was ensured by the wind turbine with a production peak of a value of 316 W. The wind turbine therefore contributes considerably to the continuity of the production of electrical energy. during night periods and days with low solar irradiation. This complementarity between wind and solar production has been shown by other authors such as R. EKE [15] and al and Ekre *et al.* [16]. They respectively worked on optimization of a wind/pv hybrid power generation system and energy system using two simulation.

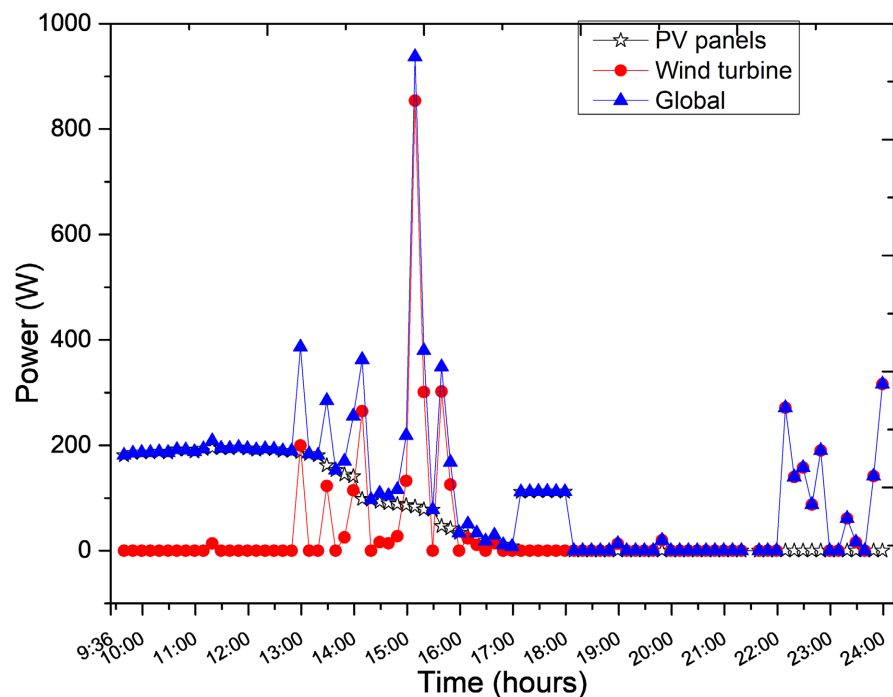


Figure 7. Evolution of the overall production of the system.

5.2. PV-Wind Turbine System Performance Optimization

For system automation, we integrate an automatic system management command through the “Arduino” programmable module. This module makes it possible to manage the three functions of the wind turbine control efficiently and automatically. The objective is to optimize the operation of the wind motor and improve the comfort of the users of the system. This mechanism is triggered automatically when the wind speed exceeds 95% of the maximum speed allowed (20 m/s) by the manufacturer through a sensor installed for this purpose. As soon as the wind speed becomes less than or equal to 95% of the maximum speed, the brake is released and the wind turbine can restart again.

Figure 8 gives an overview of the operation of the proposed command. The wind resource is represented by the rheostat. Indeed, the wind deposit is permanently

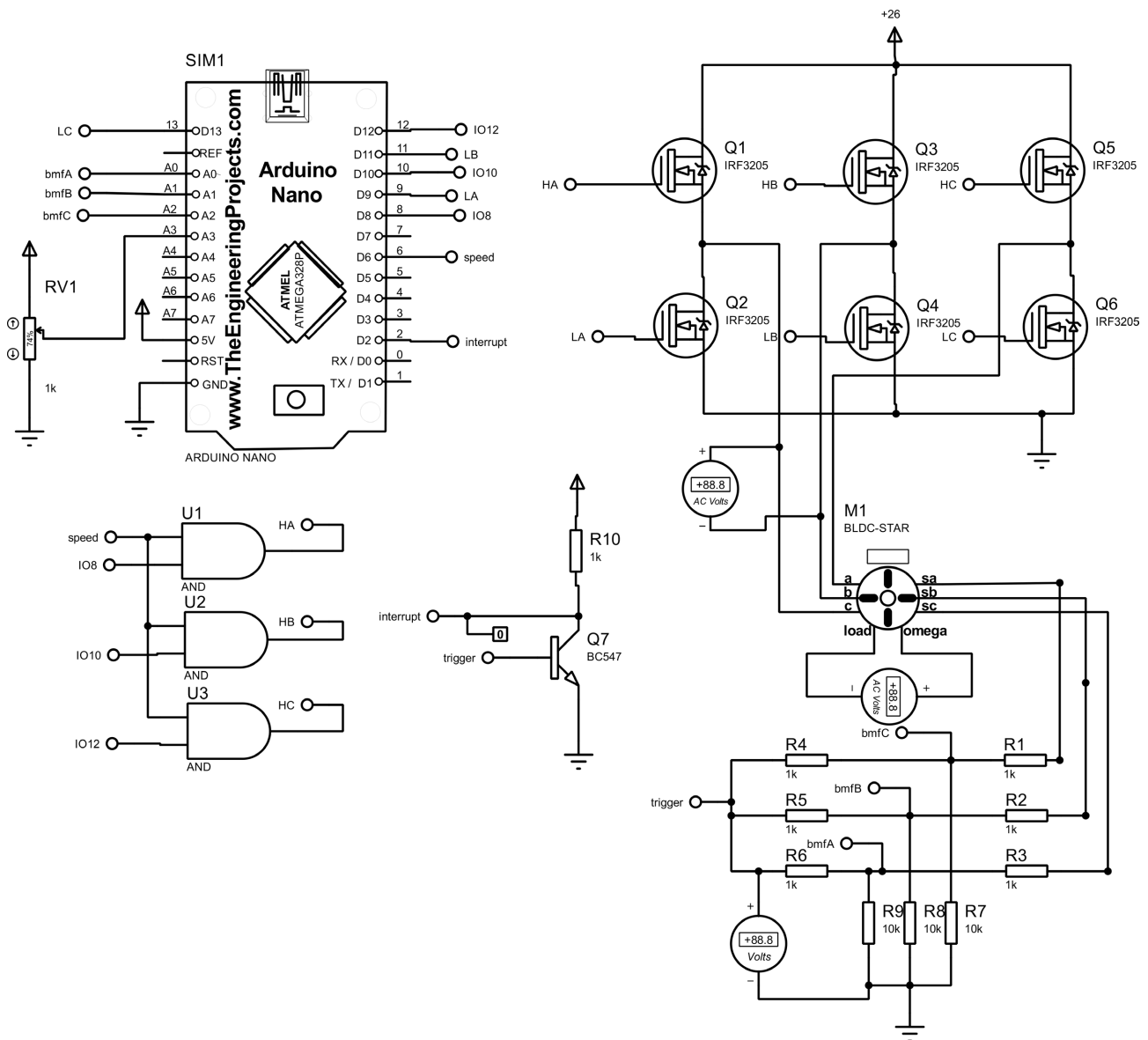


Figure 8. Synoptic diagram of the automatic control.

evaluated and transmitted to the processor in order to be analyzed. Once this action is done, the card decides to let the blades of the wind turbine turn (run position) or to block them (break position).

Figure 9 illustrates how the wind turbine works in “run” mode. As long as the wind speed is less than or equal to 95% of the maximum speed indicated by the manufacturer, that is 19 m/s. The “Arduino” management module allows the blades of the wind motor to rotate. The wind speed is evaluated and transmitted to the management module using an anemometer placed in the same plane as the wind turbine. Once the information has been received, it is processed and the processor instructs the command to execute the “run” position and the blades are free to move.

Figure 10 shows operation in the “break” position. The “break” position is activated as soon as the wind speed available at the level of the blades exceeds 95% of the maximum speed authorized by the manufacturer. As long as the wind speed is greater than 19 m/s, the processor instructs the control to short-circuit the windings of the turbine in order to block the blades of the wind turbine.

To determine the optimal height of the turbine, we exploited “Global Wind Atlas (globalwindatlas.info)”. The version used is GWA 3.0, it has a resolution of 3 km, and gives the wind speed in m/s, the power density and the probabilities of

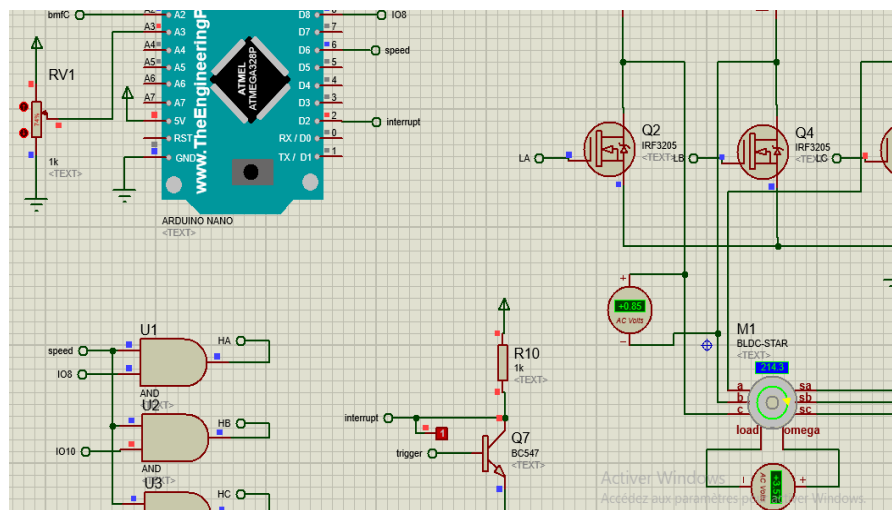


Figure 9. Simulation of wind turbine operation.

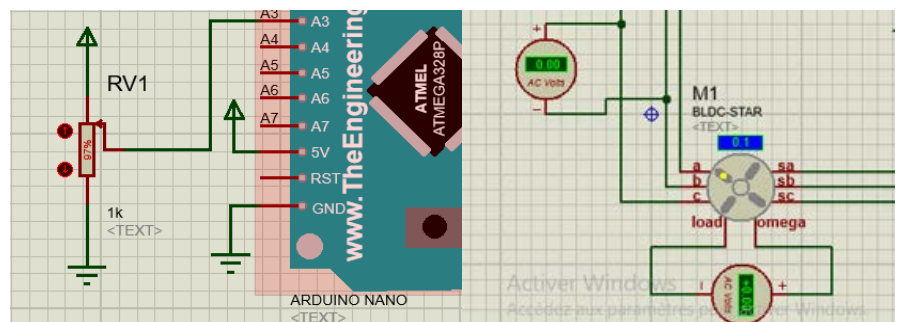


Figure 10. Simulation of wind turbine operation in the “break” position.

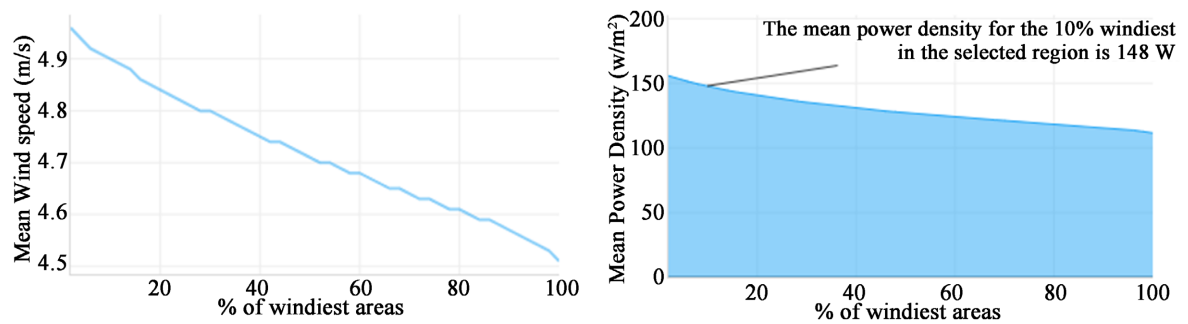


Figure 11. Power density and wind bearing at 50 m altitude.

obtaining these parameters at 10, 50, 100, 150 and 200 m above ground or sea level. For the particular case of our study, we took the data at an altitude of 50 m in Ouagadougou.

Figure 11 gives the average speeds and power densities at 50 m above the ground and the probabilities of having the values. If the turbine is installed 50 m above the ground it will produce electrical energy for at least 80% of the time because the average speed at this height is 4.61 m/s. Indeed, this speed corresponds to the speed of coupling of the shaft to the alternator of the wind turbine with a power produced of 10 W, the wind turbine will therefore produce a minimum amount of energy 70.1 kWh per year without taking account of the winter season and the harmattan period marked by good wind activity.

The power densities for the city of Ouagadougou at 50 m altitude are between 111.9 W/m² to 150 W/m² excluded. These characteristics of the deposit are very important because they guide the designer in the choice of the size of the turbine.

In view of the above, we propose that the turbine be installed at a height of thirty (30) meters above the ground. This height is optimal for the installation of domestic wind turbines in the city of Ouagadougou.

6. Conclusion

This study, which focuses on the optimization of a hybrid PV-wind energy production system, has enabled us to analyze the complementarity between solar PV production and wind turbines for self-consumption of energy for the city of Ouagadougou. It appears from this work that domestic wind turbines can be operated by combining other energy sources such as photovoltaic solar for the city of Ouagadougou. Indeed, periods of low sunshine or absence of solar deposits are generally marked by good wind activity with production that can reach 853.76 W. The investment cost of batteries represents the largest share in the financing of a photovoltaic solar system. In this sense, the operation of a domestic wind turbine at a height of 30 m above the ground can constitute an alternative to the storage of electrical energy.

Acknowledgements

We thank ISP, Uppsala University, Sweden for supporting the BUF01 project.

Conflicts of Interest

The authors declare no conflicts of interest regarding the publication of this paper.

References

- [1] Sawadogo, G.L., Igo, S.W., Compaore, A., Ouedraogo, D., Namoano, D. and Bathiebo, J.D. (2020) Modeling of Energy Savings Performed by a Barbecue Oven Isolated with Terracotta Bricks. *Physical Science International Journal*, **24**, 8-21. <https://doi.org/10.9734/psij/2020/v24i530190>
- [2] Namoano, D., Compaoré, A., Ouédraogo, O., Sawadogo, G.L., Ouedraogo, D. and Igo, S.W. (2021) Modeling Heat Transfers in a Typical Roasting Oven of Burkina Faso. *Physical Science International Journal*, **25**, 21-33. <https://doi.org/10.9734/psij/2021/v25i1130290>
- [3] Compaore, A., Ouedraogo, B., Guengane, H., Malbila, E. and Bathiebo, D.J. (2017) Role of Local Building Materials on the Energy Behaviour of Habitats in Ouagadougou. *International Journal of Applied Sciences*, **8**, 63-72. <https://doi.org/10.21013/jas.v8.n2.p3>
- [4] Boro, D., Venance Donnou, H., Kossi, I., Bado, N., Kieno, F. and Bathiebo, J. (2019) Vertical Profile of Wind Speed in the Atmospheric Boundary Layer and Assessment of Wind Resource on the Bobo Dioulasso Site in Burkina Faso. *Smart Grid and Renewable Energy*, **10**, 257-278. <https://doi.org/10.4236/sgre.2019.1011016>
- [5] Landry, M., Ouedraogo, Y. and Gagnon, Y. (2011) Atlas Éolien Du Burkina Faso. Energies Renouvelables, Production Distribuée et Communautaire. *IFDD No. 94*.
- [6] Shawon, M.J., El Chaar, L. and Lamont, L.A. (2013) Overview of Wind Energy and Its Cost in the Middle East. *Sustainable Energy Technologies and Assessment*, **2**, 1-11. <https://doi.org/10.1016/j.seta.2013.01.002>
- [7] Bambara, B. (2015) Atlas Des Energies Renouvelables. 2IE-Institut International d'Ingénierie de l'Eau et de l'Environnement, Ouagadougou.
- [8] Keyhani, A., Ghasemi-Varnamkhasti, M., Khanali, M. and Abbaszadeh, R. (2010) An Assessment of Wind Energy Potential as a Power Generation Source in the Capital of Iran, Tehran. *Energy*, **35**, 188-201. <https://doi.org/10.1016/j.energy.2009.09.009>
- [9] Qolipour, M., Mostafaeipour, A. and Rezaei, M. (2018) A Mathematical Model for Simultaneous Optimization of Renewable Electricity Price and Construction of New Wind Power Plants (Case Study: Kermanshah). *International Journal of Energy and Environmental Engineering*, **9**, 71-80. <https://doi.org/10.1007/s40095-017-0254-4>
- [10] Nair, A., Murali, K., Anbuudayasankar, S.P. and Arjunan, C.V. (2017) Modelling and Optimising the Value of a Hybrid Solar-Wind System. *IOP Conference Series: Materials Science and Engineering*, **197**, Article ID: 012035. <https://doi.org/10.1088/1757-899X/197/1/012035>
- [11] Paudel, S., Shrestha, J.N., Neto, F.J., Ferreira, J.A. and Adhikari, M. (2011) Optimization of Hybrid PV/Wind Power System for Remote Telecom Station. *IEEE International Conference on Power and Energy Systems (ICPS)*, Chennai, 22-24 December 2011, 1-6. <https://doi.org/10.1109/ICPES.2011.6156618>
- [12] Amin, B. (2015) Etude et conception d'un système hybride de production d'énergie. Université Kasdi Merbah Ouargla, Ouargla.
- [13] Merzouk N.K. and Merzouk, M. (2006) Estimation du potentiel énergétique éolien utilisable: Application au pompage dans les Hauts Plateaux. *Revue des Energies Re-*

nouvelables, **9**, 155-163.

- [14] Kapdi, R., Dahiya, R. and Naranje, V. (2016) Analysis and Optimization of Horizontal Axis Wind Turbine Blade Profile. *International Journal of Research in Engineering and Technology*, **5**, 19-24.
- [15] Eke, R., Kara, O. and Ulgen, K. (2005) Optimization of a Wind/PV Hybrid Power. *International Journal of Green Energy*, **2**, 57-63.
<https://doi.org/10.1081/GE-200051304>
- [16] Ekren, O., Ekren, B.Y. and Carriveau, R. (2011) Size Optimization of a Solar-Wind Hybrid Energy System Using Two Simulation Based Optimization Techniques. In: Carriveau, R., Ed., *Fundamental and Advanced Topics in Wind Power*, InTechOpen, London, 319-399. <https://doi.org/10.5772/18007>